INFLUENCES OF CATALYTIC TEMPERATURES AND Ru-LOADED CATALYSTS ON WASTE TIRE PYROLYSIS

Nguyen Anh Dung
Hanoi University of Mining and Geology
Email: nguyenanhdung@humg.edu.vn

Summary

This paper investigates the effects of Ru/MCM-41 catalysts in the pyrolysis of waste tire using a semi-batch reactor. The pure silica support MCM-41 was synthesised via silatrane route. Prior to evaluating the activity of Ru/MCM-41 catalysts, the influences of MCM-41 and catalytic temperature were studied. The results indicated a strong impact of MCM-41 and catalytic temperature on the yield and nature of pyrolysis products. Oil yield first decreased then increased with catalytic temperature. However, the highest catalytic temperature produced the oil having a higher poly-aromatic content. Ru/MCM-41 catalyst produced much lighter oil and dramatically decreased the concentration of poly- and polar-aromatics in the oil but also decreased the yield of oil. And the catalytic activity of Ru/MCM-41 was found to increase with Ru content in the tested range of ruthenium loading. The increase in catalytic activity was discussed in relation with catalyst characterisations.

Key words: *Pyrolysis, waste tire, bifunctional catalyst, Ru, MCM-41.*

1. Introduction

Tires are designed to be resistant to chemical, biological and physical degradation. Meanwhile, the world production of waste tire is approximately 6 x 10^6 tons/year, and nearly 70% of these waste are simply dumped in the open or in the land-filled [1, 2]. Moreover, fires at tire deposits have been reported to be very difficult to control and generate high levels of pollution to the soil, atmosphere and water [3].

Thus, over recent years, tire pyrolysis, a recycling process, has attracted significant renewed attention. It essentially involves degradation of the tire components by exposure to high temperatures in the absence of oxygen. The result is a carbonised char, condensable oil and a gas fraction. Gas fraction has been reported to have high calorific value [4], and high hydrogen content [2, 5, 6], whereas the tire-derived oil was shown to be similar, to a certain extent, to the commercial petroleum naphtha [7]. However, the high concentration of aromatic hydrocarbons (HCs) [7 - 9], especially polycyclic HCs (PAHs), has limited its application as a fuel. As a result, several studies have been done with focus on the possibilities for the production of chemical feedstock from the tire-derived oil rather than fuel. For instance, Williams and Brindle [10, 11] and Boxiong et al. [12] reported the high selectivity toward single ring aromatic HCs in the light fractions by catalytic pyrolysis of waste tire using ZSM-5 and USY zeolites as catalysts, respectively. Our previous study [13], a first step in the attempts to study the possibility of fuel production from waste tire, has shown that the mordenite-catalysed pyrolysis of waste tire produced the oil having high selectivity toward gasoline, kerosene and gas oil fractions. However, a relative high amount of poly- and polar-aromatics still existed in the oil. And the amount of aromatics increased with increasing acid properties of the catalyst. As a result, a new catalyst should be rationally designed and tested for waste tire-to-fuel process.

Bifunctional catalysts are extensively studied for aromatic reduction [14]. Metals can catalyse the hydrogenation of the feedstock, making it more reactive for cracking and heteroatom (sulfur, oxygen) removal [15]. And a high level of aromatic hydrogenation at moderate hydrogen pressures can be achieved with noble metals catalysts [16, 17]. The intrinsically high hydrogenation activity of noble metal might help reducing steric effects that impede the direct elimination of the sulfur heteroatom [18, 19]. However, noble metals display a low resistance to sulfur poisoning limiting their applications. The sulfur tolerance of a noble metal supported catalyst may be enhanced by (i) using acidic carriers [20], (ii) changing the metal particle size, or (iii) alloying with other metals [21]. Considering the metallic nature, Ru was reported to have a better sulfur tolerance than Pt, Pd or Pd-Pt catalysts in hydrogenation and ring opening of tetralin on noble metal supported on zirconium doped mesoporous silica catalysts due to the low density of states at the Fermi level of this metal [22]. Also, previous studies and the references therein on the conversion of hydrocarbons over supported and unsupported catalysts have established the order of catalytic activities for a considerable number of metals; these studies found ruthenium the most active metal investigated [23, 24]. In addition, Ru supported on

HMOR was found to exhibit higher activity in terms of PAHs removal and light oil production than other metals (Pt, Rh, Re) supported on HMOR catalysts [25] in waste tire pyrolysis. On the other hand, due to the size of the aromatic molecules, especially the PAHs, a large pore material consequently should be used as the support of the bifunctional catalyst. Pure silica MCM-41, which has a mild acidic property, was shown to exhibit good activity for the degradation of waste plastic [26 - 27]. The carbon number distribution of the derived oil shifted to lower number, and the authors also observed the carbenium ion cracking mechanism over this material [27]. Besides, catalytic temperature strongly affected the products obtained from catalytic pyrolysis of waste tire [10, 28].

The aim of this work is to investigate the influences of Ru-supported pure silica MCM-41 catalyst on the products obtained from waste tire pyrolysis. For this purpose, a pure silica MCM-41 was synthesised via silatrane route. Then, pyrolysis of waste tire using MCM-41 as a catalyst was conducted to study the effects of catalytic temperature to find the optimum condition. Subsequently, a series of Ru-supported catalysts, prepared by impregnation technique with various Ru loading, were subjected to waste tire pyrolysis to evaluate their influence on the yields and the nature of the evolved products.

2. Experiment

2.1. Catalyst preparation

To synthesise pure silica MCM-41, silatrane was first synthesised using the method of Wongkasemjit's group [29]. The silatrane precursor was added to a solution containing CTAB, NaOH, and TEA, followed by adding water with vigorous stirring [30]. The obtained crude product was filtered and washed with water to obtain a white solid. Then, the white solid was dried at room temperature and calcined at 580°C for 6 hours to obtain mesoporous MCM-41.

Ru-supported catalysts were prepared by the conventional wetness impregnation technique. An appropriate amount of precursor solution of $RuCl_3.xH_2O$ (FLUKA) was loaded to the MCM-41, followed by drying in an oven at 110°C for 3 hours, and then calcined at 580°C for 2 hours. Subsequently, it was pelletised and sieved to obtain particle sizes in the range of 400 - 425µm. Prior to the catalytic activity testing, each catalyst was reduced by hydrogen at 400°C for 3 hours.

2.2. Catalyst characterisation

XRD patterns were obtained using the Riguku D/Max 2200H with a scanning speed of 0.5 degree/min and 2θ from 1.5 degree to 60 degree. The composition of the Ru on the support was determined by the Inductively Coupled Plasma (ICP) technique using a Perkin Elmer Optima 4300 PV machine. The surface area and pore size distribution of the studied catalysts were characterised by N_2 physical adsorption using a Sorptomatic 2900 equipment. Hydrogen chemisorption at room temperature was carried out in a Micromeritics 2900 apparatus, after the in-situ reduction of sample at 500°C (10°C.min^{-1}) for 1 hour, under a flow of H_2. Dispersion data was calculated by assuming a stoichiometry H/Ru = 1 [17]. Temperature-programmed desorption (TPD) using NH_3 was carried out in a TPD/TPR Micromeritics 2900 machine. Approximately, 0.1g of sample was first pretreated in He at 550°C for 30 minutes. Then, the system was cooled to 100°C, and the NH_3 adsorption was performed using NH_3/N_2 for 1.5 hours followed by the introduction of He to remove the physically adsorbed NH_3 for 30 minutes at 100°C. Finally, the system was cooled to 50°C, and then the temperature program desorption was started from 50°C to 600°C with a heating rate of 5°C/min. TPR of Ru-supported catalysts was conducted using the same Micromeritic 2900 equipment from room temperature to 500°C with a heating rate of 5°C/min. Temperature program oxidation (TPO) using also the Micromeritics 2900 machine was performed from room temperature to 900°C (10°C/min), and the final temperature was held for 30 minutes. The amount of coke was then determined from the area under the curve and calculated by the software supplied with the machine. The catalyst characterisation was done at the Petroleum and Petrochemical College, Chulalongkorn University, Bangkok, Thailand.

2.3. Pyrolysis of waste tire

The detail of pyrolysis process was described elsewhere [13]. Briefly, the pyrolysis of waste tire was carried out in the lower zone of the reactor, where the temperature was set at 500°C. Then, the evolved product was carried by a nitrogen flow to the upper zone packed with a catalyst. This zone was controlled at various catalytic temperatures (350, 400 and 450°C) in order to investigate the influence of catalytic temperature. The obtained product was next passed through an ice-salt condensing system containing 3 condensers in order to separate incondensable compounds from the liquid product. The solid and liquid products were weighed to determine the product distribution. The

amount of gas was then determined by mass balance. Prior to being analysed, the liquid product was dissolved in n-pentane to precipitate asphaltenes. The obtained maltenes was analysed by FTIR and liquid adsorption chromatography [31]. In the later process, saturated hydrocarbons, mono-, di-, poly- and polar aromatics in the maltenes were fractionated. Finally, a Varian CP 3800 Simulated Distillation Gas Chromatograph (SIMDIST GC) equipped with FID was used to analyse the obtained maltene and hydrocarbon fractions according to the ASTM D2887 method to determine simulated true boiling point curves. The petroleum fractions were then cut based on their boiling point, including naphtha (< 200°C), kerosene (200 - 250°C), gas oil (250 - 370°C) and residue (> 370°C).

3. Results and discussion

3.1. Catalyst characterisation

Figure 1 illustrates the XRD patterns of the synthesised MCM-41 and Ru-supported samples. As seen in the figure, the structure of MCM-41 did not change after incorporation of ruthenium and no peak of ruthenium species was observed. Probably the amount of Ru loaded was below the detectable range of the XRD equipment and/or ruthenium was highly dispersed in all samples.

The physical properties of the fresh catalysts and the amount of coke of the used ones were summarised in Table 1. Accordingly, ICP analysis indicated a very good consistence between the targeted and true values of metal loaded in all samples. The BET surface area of silica MCM-41 is very high, and the average pore diameter is approximately 2.6nm, which is similar to the values reported in [30]. H_2-chemisorption results showed that the mean diameter of ruthenium particles for all samples is about 1.9nm, and the diameter increases with increasing ruthenium loading. In addition, all Ru-supported samples have a high metal dispersion of 65.2 - 68.5%. However, the dispersion of ruthenium slightly decreases with increasing concentration of ruthenium in the sample. Furthermore, the incorporation of Ru slightly decreased the surface

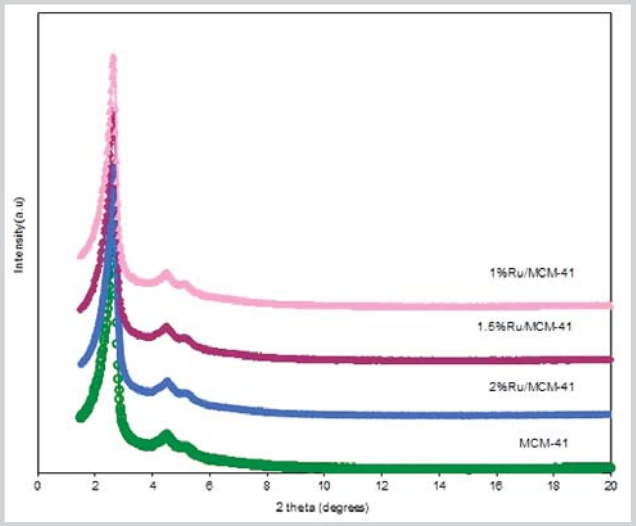

Figure 1. *XRD patterns of the MCM-41 and Ru/MCM-41 catalysts*

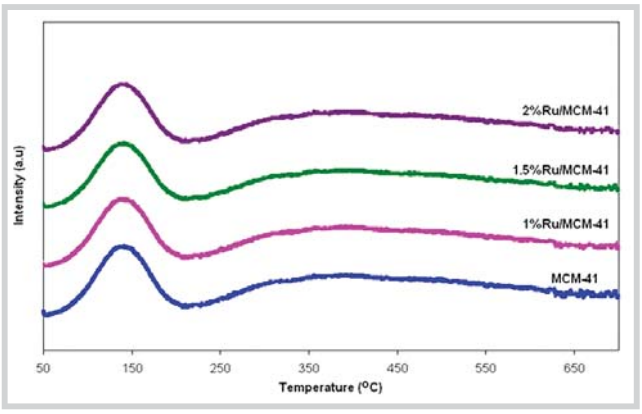

Figure 2. *TPD-NH_3 profiles of Ru/MCM-41 catalysts*

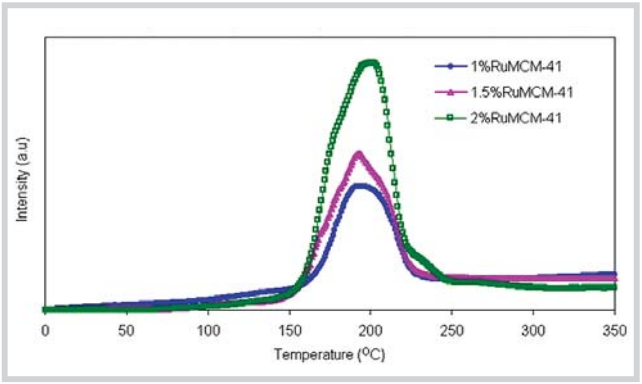

Figure 3. *TPR profiles of Ru/MCM-41 catalysts at various loading percentages*

Table 1. *Physical and chemical properties of MCM-41 and Ru-supported catalysts*

Samples	%wt Ru	Dispersion (%)	Ru particle size[b] (nm)	BET Surface area ($m^2.g^{-1}$)	Pore diameter (nm)	Coke ($g.g^{-1}$ catalyst)	Asphaltenes ($g.g^{-1}$ oil)
MCM-41 (350°C)[a]	-	-		1454	2.61	0.084	0.00064
MCM-41 (400°C)[a]	-	-		1454	2.61	0.097	0.00053
MCM-41 (450°C)[a]	-	-		1454	2.61	0.108	0.00073
1%Ru/MCM-41	0.98	68.5	1.88	1450	2.57	0.119	0.00048
1.5%Ru/MCM-41	1.51	67.9	1.90	1448	2.56	0.126	0.00041
2%Ru/MCM-41	2.02	65.2	1.98	1439	2.51	0.124	0.00022

area of the support in association with a reduction in average pore diameter, possibly caused by the diffusion of Ru into the pore.

The strength and distribution of acid sites of all prepared catalysts determined by TPD-NH_3 are given in Figure 2. It can be seen that the profile of MCM-41 shows 2 desorption peaks with maxima at 150°C and 350°C, respectively. These peaks are broad and low intensive suggesting a good distribution of the acidic sites as well as the low amount of acidic sites. As this zeolite material is composed of pure silica, the acid sites must be contributed from the silanol groups lining the wall of the channels as suggested by Seddegi et al. [27]. The incorporation of ruthenium slightly decreases the intensity of the peaks, possibly caused by the diffusion of ruthenium particles into the zeolite channels, thus blocking some acidic sites. The total acid sites of Ru-supported catalysts are comparable.

Figure 3 depicts the TPR profiles of all samples. Accordingly, the locations of the peaks in TPR profiles of all samples with different Ru loadings are similar, but the intensity increases with increasing Ru content. And, Ru-supported MCM-41 exhibits a main reduction peak at 190°C, which is higher than Ru-supported on mesoporous silica doped with zirconium [32], indicating a stronger metal support interaction. Consequently, from H_2-chemisorption analysis the high dispersion of Ru in all Ru-supported samples (> 65%) was observed (Table 1), which is well consistent with XRD results. Moreover, as indicated in Table 1, the amount of coke of the spent catalysts obtained from TPO analysis shows that Ru-supported catalysts produced a higher amount of coke than MCM-41.

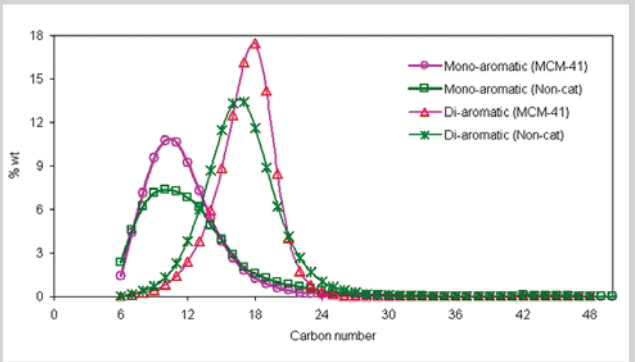

Figure 4. *Carbon number distribution of mono- and di-aromatics in oils obtained from thermal and catalytic pyrolysis using MCM-41*

3.2. Thermal and catalytic pyrolysis of waste tire

The pyrolysis products obtained from thermal and catalytic pyrolysis over MCM-41 are summarised in Table 2. It can be seen that the gas yield obtained from MCM-41 is much higher than that produced from thermal pyrolysis. In addition, with respect to thermal pyrolysis, the oil generated over MCM-41 has higher naphtha and kerosene, and the poly- and polar-aromatic contents in the oil are lower. These results might be ascribed to the cracking activity of the catalyst [13]. Besides, saturates in the derived oil decrease when using MCM-41. This is well consistent with the results obtained from FTIR analysis, as depicted in Figure 4. It can be seen that the infrared absorption bands of interest are observed around the range of C-H stretching vibration of $-CH_2-$ and $-CH_3$ groups approximately between 3,000cm^{-1} and 2,800cm^{-1} [33]. The peak at 3,030cm^{-1} represents the aromatic C-H stretching, whereas the one at 2920cm^{-1} represents the symmetric aliphatic C-H stretching, and the ratio of the two peaks correlates with the aromaticity of the hydrocarbon compounds [34]. And obviously, as compared to thermal pyrolysis, MCM-41 generated the oil having the higher ratio of I_{3030cm}-1/I_{2920cm}-1; thus, it has lower saturated hydrocarbons [33, 34].

On the other hand, the use of MCM-41 leads to a dramatic increase in the concentrations of mono- and di-aromatics (Table 2). Figure 4 illustrates the carbon number distribution of mono- and di-aromatics. Accordingly, MCM-41 causes the shifts of these compounds distribution to higher carbon number, indicating the formation of heavier aromatics. It is well accepted that aromatic hydrocarbons are not easy to be converted in a secondary cracking reaction [35, 36]. Meanwhile, alkylation reaction can be promoted by a Lewis acid catalyst [37, 38], and MCM-41 was reported to favour the alkylation reaction

Table 2. *Products obtained from thermal and catalytic pyrolysis using MCM-41**

Yield (%wt)	Non-cat	MCM-41	Content (%wt)	Non-cat	MCM-41	Yield (%wt)	Non-cat	MCM-41
Naphtha	13.02	18.81	Sat-HCs	53.81	48.21	Gas	10.33	14.56
Kerosene	8.81	9.95	Mono-aromatics	13.24	17.18	Liquid	44.02	38.02
LGO	7.80	4.83	Di-aromatics	9.88	20.37	Solid	45.65	45.42
GO	7.62	2.28	Poly-aromatics	8.99	6.55			
Residues	6.77	2.15	Polar-aromatics	12.68	7.69			

**Catalytic temperature: 350°C*

Table 3. *Pyrolysis products obtained at various catalytic temperatures*

Catalyst temperature (°C)	Product distribution (%wt)			Yields ofpetroleumcuts (%wt)				Chemicalcompositions (%wt)	
	Gas	Liquid	Solid	Naphtha	Kerosene	Gas Oil	Residues	Poly-aromatics	Polar-aromatics
Non-Cat, 350	10.33	44.02	45.65	13.02	8.81	15.42	6.77	8.99	12.68
350	14.56	38.02	45.42	18.81	9.95	7.11	2.15	6.55	7.69
400	23.52	32.05	45.24	16.49	8.38	5.88	1.11	6.45	8.05
450	13.52	42.04	44.44	15.64	10.61	13.08	2.35	8.21	11.69

of previously formed aromatic rings [39]. Therefore, it is proposed that probably MCM-41 promotes not only the cracking of saturated HCs but also the alkylation of the already-generated aromatics. As a result, heavier mono- and di-aromatics are produced, leading to the increment of mono- and di-aromatic concentration in the tire-derived oils.

3.3. Influences of catalytic temperatures

Table 3 summarises the product yields, the petroleum fractions and compositions of the oils produced by pyrolysis with MCM-41 catalyst at various catalyst temperatures. Accordingly, catalyst temperature does not influence the solid yield since the pyrolysis conditions were kept constant, and the tire was completely decomposed at 500°C [2]. However, catalyst temperature strongly affects the yields of other products. As seen from Table 3, the yield of gaseous products first increases at the expense of the liquid yield as the catalyst temperature rises from 350°C to 400°C, which is attributed to greater and deeper cracking reactions. Further increasing this temperature to 450°C causes a reduction in the yield of gaseous product in accordance with an increase in the yield of the oil. Liquid adsorption chromatography analysis also shows an increase in poly- and polar-aromatics with catalyst temperature (Table 3). Possibly, a considerable amount of olefins including conjugated olefins and aromatics, etc, produced during pyrolysis, might undergo cyclisation and alkylation followed by dehydrogenation to produce (heavier) aromatics when the acid catalyst was used [11, 40]. Note that these reactions are favoured at high reaction temperatures [6] and aromatic content in the pyrolytic oil increased when a zeolite with a large pore diameter was used [13]. Therefore, the very high catalyst temperature together with the meso-pores of the MCM-41 should be responsible for the increment of liquid yield as well as the formation of heavier aromatics from olefins and/or the lighter ones. On the other hand, it was elucidated that aromatic and alkene species have a greater predisposition to being involved in pathways to coke formation because of their ability to easily be involved in hydrogen transfer and cyclisation reactions [41]. As a result, a higher amount of coke is produced as the catalyst temperature rises (Table 1). And the high amount of coke formed can cause deactivation of the catalyst; thus, reducing its cracking activity leading to a reduction in the yield of gas product.

It can be seen in Table 3 that, regardless of the catalyst temperature, the yield of naphtha fraction from catalytic pyrolysis is higher than that from thermal pyrolysis. And the variation in catalyst temperature alters the contents of petroleum fractions in the pyrolytic oils; that is, increasing this temperature decreases naphtha in consistence with an increment in kerosene and gas oil as well as residue, suggesting the existence of the recombination of light molecules and leading to the formation of heavier compounds, and a consequent higher liquid yield. This well coincides with the fact that heavy molecules such as poly- and polar-aromatics jump up at the catalyst temperature of 450°C (Table 3). Running at the highest catalyst temperature in the testing range yields the highest amount of gas oil and kerosene. Besides, under the catalyst temperature of 400°C, the production of naphtha, kerosene and gas oil decreases, which is attributed to the high cracking activity under this condition, as mentioned previously.

Since light oils are commercially valuable, from these results together with the fact that aromatic hydrogenation is thermodynamically favoured at low temperatures [32], the catalyst temperature of 350°C was selected for further study on the effects of Ru loading.

3.4. Effects of Ru-loading amount

In this section, the effects of Ru supported on pure silica MCM-41 and the amount of Ru loading (1.0, 1.5 and 2%wt) on the yields and the nature of the products obtained from pyrolysis of waste tire were studied.

3.4.1. Product distribution

Figure 5 illustrates the effects of Ru loading amount on the product distribution. The data of MCM-41 and

non-catalytic pyrolysis were also included for comparison purpose. It can be seen that the gas yield increases dramatically at the expense of liquid yield when the catalysts were used, especially the ones with Ru loading. For instance, the gas yield obtained from pyrolysis in the absence of a catalyst is approximately 3 times less than that obtained when 2%Ru/MCM-41 was used. The promotion effects of Ru incorporation on cracking activity might be attributed to the combination of metal and acid properties of the bifunctional Ru-supported MCM-41 catalyst. The high hydrogenation activity of Ru [15] probably hydrogenated aromatic HCs, which were reported to be predominant in the products obtained from pyrolysis of waste tire [7 - 9, 11], and then these hydrogenated compounds might undergo catalytic cracking by MCM-41 producing lighter HCs. Free hydrogen is liberated from the pyrolysis products as reported in many studies [2, 5, 6], and/or is generated during the reforming reactions [2, 6]. As indicated by XRD, and H_2-chemisorption analysis, Ru is highly dispersed in all Ru-supported catalysts. The high dispersion of Ru leads not only to the formation of small Ru particles, inducing some preferential exposed planes, and then favouring hydrogenation properties [42], but also to the better transportation of the reactant/product from the acid sites to the metal sites, and vice versa [16]. That probably explains the higher cracking activity of Ru supported catalysts as compared to MCM-41. Additionally, the gas yield was found to gradually increase with increasing Ru content. 2%Ru/MCM-41 produced the highest yield of gas in line with a lowest liquid yield. This might be attributed to a good balance between metal and acid sites, as a result of the high concentration of ruthenium at approximately the same dispersion, which was reported to be a crucial factor controlling the activity of a bifunctional catalyst [43]. Also, the high activity of Ru-supported catalysts leads to a drastic reduction in asphaltenes (Table 1).

3.4.2. Pyrolytic oil

The effect of Ru loading amount can be further depicted from the petroleum cuts as shown in Figure 6. From the figure, the use of catalysts decreases gas oil and residues in accordance with the increment in the light fractions; naphtha and kerosene. The oils obtained over Ru-supported catalysts have higher content of light fractions as compared to that produced over MCM-41. This is again attributed to their bifunctionality. Moreover, the contents increase with increasing Ru loading. As compared to 1.5%Ru/MCM-41, 2%Ru/MCM-41 produces

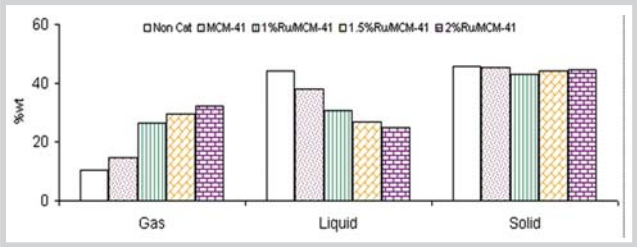

Figure 5. *Effect of Ru loading amount on product distribution*

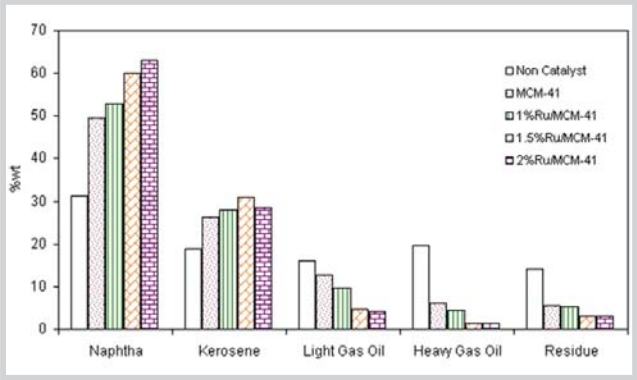

Figure 6. *Petroleum cuts of pyrolytic oils obtained from using various Ru percentages*

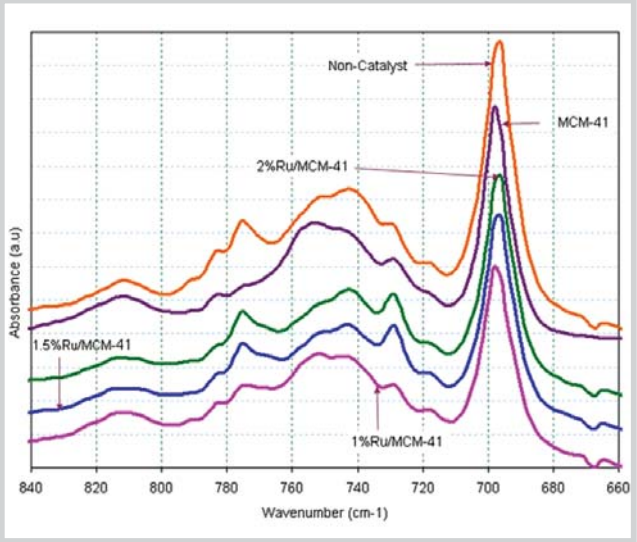

Figure 7. *IR spectra of pyrolytic oils obtained from thermal and catalytic pyrolysis*

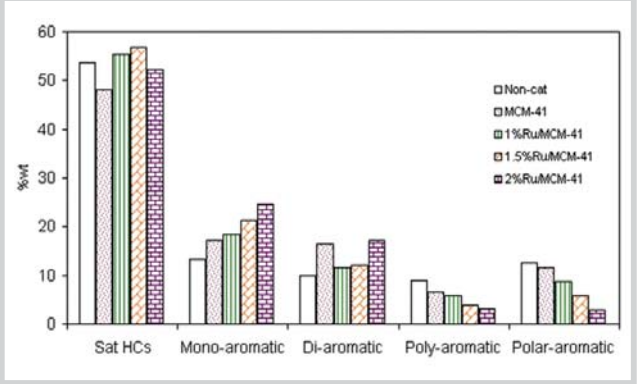

Figure 8. *The chemical compositions of pyrolytic oils obtained from thermal and catalytic pyrolysis*

the oil having slightly higher naphtha and less kerosene whereas the heavier gas oil fractions remain constant, indicating that 2%Ru/MCM-41 further cracks or transforms kerosene to naphtha and light gases.

Figure 8 illustrates the FTIR spectra of the derived oils. In the figure, bands at the wave number of 740cm^{-1} and 700cm^{-1} indicate the presence of poly-aromatics including biphenyl [32, 44]. As such, Ru-supported catalysts produce the oils having the lowest band intensity, indicating their low poly-aromatic contents. And the polycyclic aromatics decrease with increasing ruthenium loading. This is well consistent with the results obtained from liquid adsorption chromatography, as depicted in Figure 9. Besides, from the figure, a gradual increase in mono-aromatics in accordance with a decrease in poly- and polar-aromatics is observed as the ruthenium content increases. Ruthenium based catalyst was found to exhibit high hydrogenation activity [15], and its activity increased with increasing ruthenium loading [30, 45]. Akhemedov and Al-Khowaiter [46] found that Ru/ZSM-5 demonstrated much higher C-C bond cleavage selectivity in cycloalkanes in comparison with alkanes. Meanwhile, the hydrogenation of aromatics occurs mostly over the metallic function of the catalyst, although the acid sites have some hydrogenation activity [47], but the rate is considerably lower than that of metal sites [48]. It was also reported that hydrogenation of polycyclic aromatics is more preferable than single-ring aromatics [48 - 50] and generally yields partial hydrogenated products [51]. In the present study, Ru is well dispersed in all samples, as indicated by XRD, H_2-chemisorption analysis. Therefore, it is likely that increasing Ru loading benefits a higher hydrogenation activity, promoting conversion of poly-aromatics to (partial) hydrogenated compounds, which would further undergo ring-opening and/or cracking over acid sites. As a consequence, higher concentration of mono-aromatics and light fractions are achieved.

On the other hand, the increasing ruthenium loading also leads to the gradual reduction in polar-aromatics (Figure 8). Several explanations might be extended to explain the polar-aromatic reduction having occurred in the cases of Ru-supported catalysts. The increasing ruthenium content would prevent polar-aromatic formation due to the enhanced hydrogenation activity [52]. At the same time, side cracking reaction that produces polar-aromatics with lower molecular weights [53, 54] might also be a candidate. And, the high amount of coke generated on the spent Ru-supported catalysts (Table 1) as a result of the accumulation of polar-aromatic compounds [53] should not be excluded. Besides, the increase in hydrogenation activity with increasing ruthenium content in the catalyst might promote the hydrodesulfurisation (HDS) reactions, causing the reduction of polar-aromatics. This is more likely to occur since the HDS of the feed containing both polar-aromatics and other polycyclic aromatics mainly followed the HYD pathway due to the competition adsorption on the active sites [55]. And, it is also well-known that the HDS reactions via HYD pathway lead to the formation of mono-aromatic [56]. That probably explains the gradual increase in mono-aromatics at the expense of polar-aromatics as observed in Figure 8.

Finally, the reason for a high concentration of di-aromatics in the oil obtained over 2%Ru/MCM-41 (Figure 8) is not clear. However, from the FTIR analysis (Figure 7, the bands at the wave number of around 700cm^{-1}), it seems that the high di-aromatics content might be attributed, or at least partially, to the high concentration of bi-phenyl and its substituted compounds [47]. Therefore, it is possible that the presence of high amount of Ru sites on the very large surface of MCM-41, to a certain extent, decreases the steric hindrance, resulting in a promotion effect on the occurrence of the HDS reaction via DDS route, which is well known to produce di-aromatics [56]. Pawelec et al. [57] found that the HDS of 4,6 dimethyl-dibenzothiophene on CoMo/P/Ti-HMS (Hexagonal Mesoporous Silica material_HMS) catalysts occurred via (i) dealkylation, resulting in dibenzothiophene formation; and (ii) isomerisation (main route) to produce 3,6 dimethyl-DBT, and eventually 3,4' dimethyl-biphenyl and 3,4' methylcyclohexyl toluene products. However, no study on Ru-supported pure silica MCM-41 have been published for the ability of this catalyst to drive the HDS of 4,6 dimethyl-DBT via the isomerisation route as introduced by Pawelec [57]. But, to study this is out of the scope of this research work. Therefore, a further study is needed to elucidate this issue.

4. Conclusions

Catalytic temperatures strongly influenced the product distribution and the nature of the products obtained from the MCM-41 catalysed-pyrolysis of waste tire. The oil yield first decreased, and then increased with catalyst temperature. Under the highest studied catalyst temperature, the highest poly- and polar-aromatics were

produced. In addition, increasing catalyst temperature decreased the yield of naphtha in accordance with the increment of heavier fractions. These phenomena might be attributed to the combination effects of high catalyst temperature, the meso-pore and acid properties of MCM-41, leading to the preference occurrence of alkylation, aromatisation and Diel-Alder reactions.

Ru was highly dispersed in all Ru-supported catalysts. The incorporation of Ru on the surface of MCM-41 was found to have promotion effects on the catalytic activity. And the catalytic activity increased with increasing Ru loading, which was attributed to a better hydrogenation activity. Gas yield gradually increased at the expense of the liquid yields with Ru content in the bifunctional catalysts. Furthermore, Ru-supported catalysts produced much lighter oils as compared to MCM-41 and non-catalytic pyrolysis. A higher selectivity toward light petroleum fractions was also observed over a catalyst having higher concentration of ruthenium metal sites. That was explained by the promotion in the hydrogenation of both poly- and polar-aromatics, as Ru loading increased, followed by ring-opening and/or cracking producing lower molecular weight hydrocarbons.

References

1. S.Galvagno, S.Casu, T.Casabianca, A.Calabrese, G.Cornacchia. *Pyrolysis process for the treatment of scrap tyres: preliminary experimental results*. Waste Management. 2002; 22(8): p. 917 - 923.

2. C.Berrueco, E.Esperanza, F.J.Mastral, J.Ceamanos. P.García-Baicaicoa. *Pyrolysis of waste tyres in an atmospheric static-bed batch reactor: Analysis of the gases obtained*. Journal of Analytical and Applied Pyrolysis. 2005; 74(1 - 2): p. 245 - 253.

3. UK Environment Agency. *Tires in the environment*. 1998.

4. Mahmood M.Barbooti, Thamer J.Mohamed, Alla A.Hussain, Falak O.Abas. *Optimization of pyrolysis conditions of scrap tires under inert gas atmosphere.* Journal of Analytical and Applied Pyrolysis. 2004; 72(1): p. 165 - 170.

5. E.Aylón, R.Murillo, A.Fernández-Colino, A.Aranda, T.García, M.S.Callén, A.M.Mastral. *Emissions from the combustion of gas-phase products at tyre pyrolysis*. Journal of Analytical and Applied Pyrolysis. 2007; 79(1 - 2): p. 210 - 214.

6. Paul T.Williams, David T.Taylor. *Aromatization of tyre pyrolysis oil to yield polycyclic aromatic hydrocarbons*. Fuel. 1993; 72(11): p. 1469 - 1474.

7. B.Benallal, C.Roy, H.Pakdel, S.Chabot, M.A.Poirier. *Characterization of pyrolytic light naphtha from vacuum pyrolysis of used tyres comparison with petroleum naphtha*. Fuel. 1995; 74(11): p. 1589 - 1594.

8. Adrian M.Cunliffe, Paul T.Williams. *Composition of oils derived from the batch pyrolysis of tyres*. Journal of Analytical and Applied Pyrolysis. 1998; 44(2): p. 131 - 152.

9. Paul T.Williams, Richard P.Bottrill. *Sulfur-polycyclic aromatic hydrocarbons in tyre pyrolysis oil*. Fuel. 1995; 74(5): p. 736 - 742.

10. P.T.Williams, A.J.Brindle. *Catalytic pyrolysis of tyres: influence of catalyst temperature*. Fuel. 2002; 81(18): p. 2425 - 2434.

11. P.T.Williams, A.J.Brindle. *Aromatic chemicals from the catalytic pyrolysis of scrap tyres*. Journal of Analytical and Applied Pyrolysis. 2003; 67(1): p. 143 - 164.

12. S.Boxiong, W.Chunfei, G.Binbin, W.Rui, Liangcai. *Pyrolysis of waste tyres with zeolite USY and ZSM-5 catalysts*. Applied Catalysis B: Environmental. 24 2007; 73(1 - 2): p. 150 - 157.

13. N.A.Dung, A.Mhodmonthin, S.Wongkasemjit, S.Jitkarnka. *Effects of ITQ-21 and ITQ-24 as zeolite additives on the oil products obtained from the catalytic pyrolysis of waste tire.* Journal of Analytical and Applied Pyrolysis. 2009; 85(1 - 2): p. 338 - 344.

14. Alois Lugstein, Andreas Jentys, Hannelore Vinek. *Hydroisomerization and cracking of n-octane and C8 isomers on Ni-containing zeolites*. Applied Catalysis A: General. 1999; 176(1): p.119 - 128.

15. M.A.Ali, T.Kimura, Y.Suzuki, M.A.Al-Saleh, H.Hamid, T.Inui. *Hydrogen spillover phenomenon in noble metal modified clay-based hydrocracking catalysts*. Applied Catalysis A: General. 2002; 277(1 - 2): p. 63 - 72.

16. D.Eliche-Quesada, J.M.Meria-Robles. E.Rodriguez-Castellon, A.Jimenez-Lopez. *Influence of the incorporation of palladium on Ru/MCM hydrotreating catalysts*. Applied Catalysis B: Environmental. 2006; 65(1 - 2): p.118 - 126.

17. D.Eliche-Quesada, M.I.Macias-Ortiz, J.Jimenez-Jimenez, E.Rodriguez-Castellon, J.Jimenez-Lopez. *Catalysts based on Ru/mesoporous phosphate heterostructures (PPH) for hydrotreating of aromatic hydrocarbons*. Journal of Molecular Catalysis A: Chemical. 2006; 225(1 - 2): p. 41 - 48.

18. J.B.McKinley. *Catalysis*. New York: Reinhold. 1957.

19. T.A.Pecoraro, R.R.Chianelli. *Hydrodesulfurization catalysis by transition metal sulfides*. Journal of Catalysis. 1981; 67: p. 430 - 445.

20. J.Barbier, E.Lamy-Pitara, P.Marecot, J.P.Boitiaux, J.Cosyns, F.Verna. *Role of sulfur in catalytic hydrogenation reactions*. Advances in Catalysis. 1990; 37: p. 279 - 318.

21. Joeng-Kyu Lee, Hyun-Ku Rhee. *Sulfur tolerance of zeolite beta-supported Pd-Pt catalysts for the isomerization of n-hexane*. Journal of Catalysis. 1998; 177: p. 208 - 216.

22. E.Rodriguez-Castellon, J.Merida-Robles, L.Diaz, P.Maireles-Torres, J.J.Jones, J.Roziere, A. Jimenez-Lopez. *Hydrogenation and ring opening of tetralin on noble metal supported on zirconium doped mesoporous silica catalysts*. Applied. Catalysis. A: General. 2004; 260: p. 9 - 18.

23. S.Gao, L.D.Schmidt. *Effect of oxidation-reduction cycling on C_2H_6 hydrogenolysis: Comparison of Ru, Rh, Ir, Ni, Pt, and Pd on SiO_2*. Journal of Catalysis. 1989; 115(2): p. 356 - 364.

24. Vagif M.Akhmedov, S.H.Al-Khowaiter. *Hydro-conversion of hydrocarbons over Ru-containing supported catalysts prepared by metal vapor method*. Applied Catalysis A: General. 2000; 197(2): p. 201 - 212.

25. Nguyen Anh Dung. *Catalytic pyrolysis of waste tire using noble metals-supported HMOR catalysts*. Petrovietnam Journal. 2015; 6: p. 43 - 50.

26. M.A.Uddin, Y.Sakata, A.Muto, Y.Shiraga, K.Koizumi, Y.Kanada, K.Murata. *Catalytic degradation of polyethylene and polypropylene into liquid hydrocarbons with mesoporous silica*. Microporous and Mesoporous Materials. 1998; 21: p. 557 - 564.

27. Z.S.Seddegi, U.Budrthumal, A.A.Al-Arfaj, A.M.Al-Amer, S.A.I.Barri. *Catalytic cracking of polyethylene over all-silica MCM-41 molecular sieve*. Applied Catalysis A: General. 2002; 225: p. 167 - 176.

28. Boxiong Shen, Chunfei Wu, Rui Wang, Binbin Guo, Cai Liang. *Pyrolysis of scrap tyres with zeolite USY*. Journal of Hazardous Materials. 2006; 137: p. 1065 - 1073.

29. W.Charoenpinijkarn, M.Suwankruhasn, B.Kesapabutr, S.Wongkasemjit, A.M.Jamieson. *Sol-gel processing of silatranes*. European Polymer Journal. 2001; 37(7): p. 1441 - 1448.

30. N.Thanabodeekij, S.Sadthayanon, E.Gulari, S.Wongkasemjit. *Extremely high surface area of ordered mesoporous MCM-41 by atrane route*. Materials Chemistry and Physics. 2006; 98: p. 131 - 137.

31. G.Sebor, J.Blazek, M.F.Nemer. *Optimization of the preparative separation of petroleum maltenes by liquid adsorption chromatography*. Journal of Chromatography A. 1999; 847: p. 323 - 330.

32. Eliche-Quesada, J.M.Merida-Robles, E. Rodríguez-Castellon, A. Jiménez-Lopez. *Ru, Os and Ru-Os supported on mesoporous silica doped with zirconium as mild thio-tolerant catalysts in the hydrogenation and hydrogenolysis/hydrocracking of tetralin*. Applied Catalysis A: General. 2005; 279(1 - 2): p. 209 - 221.

33. S.H.Wang, P.R.Griffiths. *Resolution enhancement of diffuse reflectance i.r. spectra of coals by Fourier self-deconvolution: 1. C-H stretching and bending modes*. Fuel. 1985; 64: p. 229 - 236.

34. C.A.Islas-Flores, E.Buenrostro-Gonzalez, C.Lira-Galeana. *Fractionation of petroleum resins by normal and reverse phase liquid chromatography*. Fuel. 2006; 85: p. 1842 - 1850.

35. Z. Liu, X. Meng, C. Xu, J. Gao *Secondary cracking of gasoline and diesel from heavy oil catalytic pyrolysis*. Chinese Journal of Chemical Engineering. 2007; 15(3): p. 309 - 314.

36. X.Meng, C.Xu, J.Gao, Lili. *Studies on catalytic pyrolysis of heavy oils: Reaction behaviors and mechanistic pathways*. Applied Catalysis A: General. 2005; 294(2): p. 168 - 176.

37. John J.McKetta. *Chemical processing handbook*. CRC Press. 1993.

38. Z.Zhao, W.Qiao, X.Wang, G.Wang, Z.Li, L.Cheng. *Effect of alkaline earth metals on catalytic performance of HY zeolite for alkylation of α-methylnaphthalene with long-chain olefins*. Microporous and Mesoporous Materials. 2006; 94(1 - 3): p. 105 - 112.

39. G.San Miguel, J.Aguado, D.P.Serrano, J.M.Escola. *Thermal and catalytic conversion of used tyre rubber and its polymeric constituents using Py-GC/MS*. Applied Catalysis B: Environmental. 2 May 2006; 64(3 - 4): p. 209 - 219.

40. K.H.Lee, Y.W.Lee, B.H.Ha. *Catalytic cracking of vacuum gas oil on the dealuminated mordenites*. Journal of Catalysis. 1998; 178(1): p. 328 - 337.

41. P.B.Venuto, T.E.Habib. *Fluid catalytic cracking with zeolite catalysts*. Marcel Dekker, New York. 1979.

42. R.M.Navarro, P.Castaño, M.C.Álvarez-Galván, B.Pawelec. *Hydrodesulfurization of dibenzothiophene and a SRGO on sulfide Ni(Co)Mo/Al$_2$O$_3$ catalysts. Effect of Ru and Pd promotion*. Catalysis Today. 2009; 143(1 - 2): p. 108 - 114.

43. A. Soualah, J.L. Lemberton, L. Pinard, M. Chater, P. Magnoux, K. Moljord. *Hydroisomerization of long-chain n-alkanes on bifunctional Pt/zeolite catalysts: Effect of the zeolite structure on the product selectivity and on the reaction mechanism*. Applied Catalysis A: General. 2008; 336(1 - 2): p. 23 - 28.

44. C.Jäger, F.Huisken, H.Mutschke, Th.Henning, W.Poppitz, I.Voicu. *Identification and spectral properties of PAHs in carbonaceous material produced by laser pyrolysis*. Carbon. 2007; 45(15): p. 2981 - 2994.

45. D.Eliche-Quesada, E.Rodríguez-Castellón, A.Jiménez-López. *Hydrodesulfurization activity over supported sulfided ruthenium catalysts. Influence of the support*. Microporous and Mesoporous Materials. 2007; 99(3): p. 268 - 278.

46. V.M.Akhmedov, S.H.Al-Khowaiter. *Hydroconversion of hydrocarbons over Ru-containing supported catalysts prepared by metal vapor method*. Applied Catalysis A: General. 2000; 197(2): p. 201 - 212.

47. O.Cairon, K.Thomas, A.Chambellan, T.Chevreau. *Acid-catalysed benzene hydroconversion using various zeolites: Brönsted acidity, hydrogenation and side-reactions*. Applied Catalysis A: General. 2003; 238(2): p. 167 - 183.

48. P.Castano, B.Pawelec, J.L.G.Fierro, J.M.Arandes, J.Bilbao. *Aromatics reduction of pyrolysis gasoline (PyGas) over HY-supported transition metal catalysts.* Applied Catalysis A: General. 2006; 315: p. 101 - 113.

49. A.Corma, A.Martínez, V.Martínez-Soria. *Hydrogenation of aromatics in diesel fuels on Pt/MCM-41 Catalysts*. Journal of Catalysis. 1997; 169(2): p. 480 - 489.

50. S.Jongpatiwut, Z.Li, D.E.Resasco, W.E.Alvarez, E.L. Sughrue, G.W.Dodwell. *Competitive hydrogenation of poly-aromatic hydrocarbons on sulfur-resistant bimetallic Pt-Pd catalysts*. Applied Catalysis A: General. 2004; 262(2): p. 241 - 253.

51. M.Jacquin, D.J.Jones, J.Roziere, S.Albertazzi, A.Vaccari, M.Lenarda, L.Storaro, R.Ganzerla. *Novel supported Rh, Pt, Ir and Ru mesoporous aluminosilicates as catalysts for the hydrogenation of naphthalene*. Applied Catalysis A: General. 2003; 251(1): p. 131 - 141.

52. N.A. Dung, R. Klaewkla, S. Wongkasemjit, S. Jitkarnka. *Light olefins and light oil production from catalytic pyrolysis of waste tire.* Journal of Analytical and Applied Pyrolysis. 2009; 86(2): p. 281 - 286.

53. A.Corma, C.Martinez, G.Ketley, G.Blair. *On the mechanism of sulfur removal during catalytic cracking*. Applied Catalysis A: General. 2001; 208(1 - 2): p. 135 - 152.

54. J.A.Valla, A.A.Lappas, I.A.Vasalos. *Catalytic cracking of thiophene and benzothiophene: Mechanism and kinetics*. Applied Catalysis A: General. 2006; 297(1): p. 90 - 101.

55. H.Pakdel. D.M.Pantea, C.Roy. *Production of Dl-limonene by vacuum pyrolysis of used tires*. Journal of Analytical and Applied Pyrolysis. 2001; 57(1): p. 91 - 107.

56. H.Wang, R.Prins. *Hydrodesulfurization of dibenzothiophene and its hydrogenated intermediates over sulfided Mo/γ-Al$_2$O$_3$*. Journal of Catalysis. 2008; 258(1): p. 153 - 164.

57. B.Pawelec, J.L.G.Fierro, A.Montesinos, T.A.Zepeda. *Influence of the acidity of nanostructured CoMo/P/Ti-HMS catalysts on the HDS of 4,6-DMDBT reaction pathways.* Applied Catalysis B: Environmental. 2008; 80(1 - 2): p. 1 - 14.